Search for reflection asymmetric structures in the $A=145$ mass region: Decays of 1.8-s ^{143}Cs to levels of ^{143}Ba and 4.1-s ^{147}La to levels of ^{147}Ce

J. D. Robertson,* P. F. Mantica, Jr., S. H. Faller,† C. A. Stone,‡
E. M. Baum*, and W. B. Walters
Department of Chemistry, University of Maryland, College Park, Maryland 20742
(Received 5 July 1989)

The level structures of ^{143}Ba and ^{147}Ce have been investigated by studying the β decays of 1.8-s ^{143}Cs and 4.1-s ^{147}La to search for evidence of intrinsic reflection asymmetry in light rare-earth nuclei. Gamma-ray energies and relative intensity values, γ-γ coincidence intensities, and γ-γ angular correlation coefficients were measured. The parity doublets that characterize reflection asymmetric rotational structures in the light odd-A actinides were not readily identified in ^{143}Ba or ^{147}Ce. The observed level structures, combined with other data for these nuclides, suggest that weak deformation is present and that reflection asymmetric admixtures may play a significant role in driving that deformation.

I. INTRODUCTION

Recently, Leander *et al.*[1] proposed that nuclei with $N=86-90$ with mass and charge near that of ^{145}Ba may form a new region of reflection asymmetric deformation similar to that which is observed in the $Z=88-90$ light odd-A actinide region. Subsequent investigation by Robertson *et al.* of the structure of ^{145}Ba via the β decay of ^{145}Cs did not reveal strong evidence for the idea that ^{145}Ba breaks reflection symmetry in the intrinsic frame.[2] The parity doublets which characterize the octupole-deformed light odd-A actinides were not observed at low energies in ^{145}Ba. (In this work we equate the terms reflection-asymmetric deformation and octupole deformation. Moreover, the term octupole deformation can also imply the idea of a dipole cluster.) The results of this study did suggest, however, that reflection-asymmetric correlations may play a role in determining the low-lying structure in this region. Recently, more experimental support was obtained for this conclusion by the observation of alternating-parity rotational bands at high spins in ^{144,146}Ba and ^{146}Ce by Phillips *et al.*[3,4] and in ^{148,150}Sm and ^{146,148}Nd by Urban *et al.*[5,6] These rotational bands, which resemble those observed at low energies in the light actinide region, indicate that the neutron-rich Ba, Ce, Nd, and Sm isotopes acquire an octupole-deformed shape at high spins. Unfortunately, the strength of the reflection-asymmetric correlations and their specific effects on the low-lying structure in this region could not be determined by examining a single, isolated case. An investigation of the structure of ^{143}Ba and ^{147}Ce via the β decay of ^{143}Cs and ^{147}La has been undertaken in order to better characterize these nuclides outside the doubly closed ^{132}Sn shell that are near ^{145}Ba. The study of ^{143}Ba provides additional data for the systematics of the $Z=56$ isotopes from the $N=82$ neutron shell to ^{145}Ba and the study of ^{147}Ce provides additional data for the systematics of the $N=89$ isotones from the $Z=64$ subshell to ^{145}Ba.

The ground state spin, spectroscopic quadrupole moment, and magnetic dipole moment of ^{143}Ba have been measured by collinear fast beam laser spectroscopy.[7] The structure of ^{143}Ba was first investigated by Schussler *et al.*[8] Their study of the decay of ^{143}Cs included γ-ray singles, γ-γ coincidence, β-γ coincidence, and conversion electron (CE) measurements. Recently, Rapaport and Gayer have reexamined part of the work of Schussler *et al.* by measuring the γ-ray singles and conversion electrons from ^{143}Cs decay.[9] Although the works of Schussler *et al.* and Rapaport and Gayer are in reasonable agreement, only tentative spins and parities were assigned to the excited states in ^{143}Ba based upon the $\frac{5}{2}$ ground state spin and the measured transition multipolarities. Because the CE measurements of the previous works agree, only γ singles, γ-γ coincidence, and γ-γ angular correlation measurements were made in our study of ^{143}Cs decay.

The structure of ^{147}Ce was first studied by Blachot *et al.*[10] in 1977. Two later investigations of the decay of ^{147}La were presented at the 4th International Conference on Nuclei Far From Stability.[11,12] The decay schemes presented in both of these studies support and expand the previous work by Blachot *et al.*, but are not themselves in good agreement. The most serious discrepancy involves a level at 215 keV reported by Schussler *et al.*[12] that is not in the decay scheme reported by Shmid *et al.*[11] Other major differences in the two works are levels at 359, 433, 608, 673, 677, and 710 keV in the decay scheme proposed by Schussler *et al.* that are not reported in the level scheme of Shmid *et al.* An investigation of the β decay of 4.2-s ^{147}La into levels of ^{147}Ce has been undertaken in order to resolve these discrepancies. Because the activity of the ^{147}La samples was too low for γ-γ angular correlation measurements, the ^{147}Ce study only involved γ-ray singles and γ-γ coincidence measurements.

II. EXPERIMENTAL PROCEDURE

The investigations of the β decay of ^{143}Cs and ^{147}La were conducted at the mass separator TRISTAN on-line to the high flux beam reactor at Brookhaven National Laboratory.[13] The radioactive samples were produced by

thermal-neutron induced fission of a ^{235}U target integrated in a positive surface ionization (PSI) source.[14] A Re ionizer was used in the PSI source for the ^{147}La study and a Ta ionizer was used in the PSI source for the ^{143}Cs study. The lower work function of Ta (compared to Re) ensured no independent production of Ba from the ion source at low-power operation ($T \approx 1200$ °C).

In all of the γ-ray measurements, the radioactive beams were deposited on an aluminized Mylar tape in a moving-tape collection (MTC) system. For the ^{143}Cs decay studies, the radioactive samples were simultaneously deposited and counted at the parent port of the MTC. In order to reduce the amount of Ba daughter activity in the samples, the tape was cycled every three seconds to remove the builtup daughter ^{143}Ba activity. For the ^{147}La study, the radioactive samples were produced by separating the ^{147}Cs grandparent and the ^{147}Ba parent. The mass-separated beam was first deposited at the parent port of the MTC for four seconds to produce a saturated sample of 0.2-s ^{147}Cs and 0.7-s ^{147}Ba. This sample was then moved to a shielded position halfway to the daughter port of the MTC and allowed to decay for four seconds. The sample, in which ^{147}La now accounts for over 95% of the total activity, was then moved to the daughter port and counted for four seconds.

Two Ge(Li) and two Ge detectors were used to collect the gamma singles and γ-γ coincidence data. The two coaxial Ge detectors were a 90-cm^3 Ge(Li) with full width at half maximum (FWHM) of 2.2 keV at 1.33 MeV and a 79-cm^3 Ge(Li) with FWHM of 2.4 keV at 1.33 MeV. The two coaxial Ge detectors were a 76-cm^3 Ge with FWHM of 2.2 keV at 1.33 MeV and a 79-cm^3 Ge with FWHM of 1.9 keV at 1.33 MeV. In addition, a 2-cm^3 planar Ge detector with a FWHM of 0.55 keV at 122 keV was used to measure low-energy γ rays.

In the ^{143}Cs decay study, high-energy (0–2 MeV) and low-energy (0–500 keV) γ-ray singles spectra were acquired with one Ge detector and the planar Ge detector. For the γ-γ coincidence and angular correlation measurements, the four γ-ray detectors were placed around the parent port 7.5 cm from the radioactive source. Two angles were measured by the four detectors (six detector pairs): four points at 90° and two points at 180°. The angular correlations for the gamma rays in the two $0^+(E2)2^+(E2)0^+$ cascades in the decay of ^{142}Cs to ^{142}Ba were used to calibrate the four detector system. The $A=142$ activity was adjusted to be approximately equal to that of the $A=143$ samples. A total of 3×10^7 three parameter $\gamma\gamma t$ coincidence events were collected in the ^{143}Cs experiment.

In a separate experiment, the population of the levels of ^{143}Ba was observed following the decay of ^{144}Cs by delayed neutron emission. This study was performed by collecting γ-ray singles spectra to energies of 3 MeV using a Ge detector. Because the ground state spin and parity of ^{144}Cs are 1^-, excited levels with spins and parities of 0^-, 1^-, and 2^- in ^{144}Ba will be populated in the decay of ^{144}Cs. The subsequent decay of these levels by s-wave neutrons will, in turn, directly populate low-energy $\frac{1}{2}^-$, $\frac{3}{2}^-$, and $\frac{5}{2}^-$ levels in ^{143}Ba. With a difference between Q_β and S_n of approximately 2 MeV, levels up to that energy could be populated in delayed-neutron emission. We, however, only observed γ rays up to 873 keV that could be assigned to levels in ^{143}Ba.

For the ^{147}La decay study, high-energy (0–4.5 MeV) and intermediate-energy (0–2 MeV) γ-ray singles spectra were acquired with the 90-cm^3 Ge(Li) detector and one Ge detector. In addition, a low-energy (0–500 keV) γ-ray singles spectrum was acquired with the planar Ge detector. Because of the low activity of the ^{147}La samples, one of the Ge detectors and the planar detector were placed at a source-to-detector distance of 3.8 cm and the second Ge detector was placed at a distance of 7.6 cm. A total of 1×10^7 three parameter $\gamma\gamma t$ coincidence events were collected in the ^{147}Ce experiment.

III. ^{143}Ba EXPERIMENTAL RESULTS

A. Gamma-ray energies and intensities

The γ rays assigned to ^{143}Cs decay are given in Table I. The assignments are based upon the appearance of the γ ray in (1) the singles spectra and (2) the coincidence spectra gated on the strongest transitions which have been previously assigned to ^{143}Cs decay.[15] The results from the coincidence scans are shown in Table II. The contributions of the ^{143}Ba daughter γ rays to the ^{143}Cs singles spectra were removed using the intensity values reported by Faller *et al.*[16] For the majority of the γ rays listed in Table I, the energy and intensity values were determined from the singles data. In several cases, however, it was impossible to ascertain this information from the singles spectra because the intensity of the transition was too low or the γ ray was a member of a complex multiplet. In these instances, the energy and/or intensity values were determined from the coincidence spectra.

In general, the agreement between this work and that of Schussler *et al.*[8] and Rapaport and Gayer[9] is quite good and most of the discrepancies between the two earlier works have been resolved. The present work confirms the observation by Rapaport and Gayer of two transitions at 480 and 515 keV. Also, in agreement with Rapaport and Gayer, we did not observe the γ rays at 524, 595, 653, 682, 743, 911, and 969 keV which were reported by Schussler *et al.* On the other hand, we did observe and place the 712- and 1154-keV γ rays which were reported by Schussler *et al.* In contrast to both previous works, no evidence was found either in singles or coincidence for the 198-keV transition. Furthermore, the gain of the detectors limited the maximum energy observed to 1.8 MeV so that we did not observe the three γ-ray transitions reported above 1.8 MeV. Twenty new transitions have been assigned to the decay of ^{143}Cs. Thirteen of these new γ rays were observed in the coincidence spectra and placed in the decay scheme. Of the remaining seven, five were placed feeding into the ground state and 33-keV level based upon energy sum relationships.

B. Angular correlation measurements

The results of the angular correlation study are given in Table III. For each cascade we report an A_{22} value

TABLE I. Gamma rays assigned to the decay of ^{143}Cs.

Energy (keV)[a]	Intensity[b]		Placement		Multipolarity[c]
	^{143}Cs decay	^{144}Cs decay	From	To	
33.46	2.3(2)		33	0	*E*2
74.13[d]	1.2(1)		307	233	
77.75	0.3(1)		307	229	
117.32(5)	9.7(4)	10.4(7)	117	0	*E*2
146.00(3)	3.2(2)	2.5(7)	263	117	*M*1/*E*2
160.00(5)	3.5(2)	1.7(8)	467	307	*M*1/*E*2
195.26(6)	100	100	229	33	*M*1/*E*2
204.3(1)	0.6(1)				
228.80(6)[e]	20(1)	0.7(2)	229	0	*M*1/*E*2
232.52(2)	66(2)	81(4)	233	0	*M*1/*E*2
234.2(1)[d,f]	2.0(2)		467	233	
237.93(4)	3.1(8)	3.6(2)	467	229	
263.46(3)	29(1)	37(2)	263	0	*M*1/*E*2
273.18(4)	34(1)	35(1)	307	33	*M*1/*E*2
299.33(5)	6.4(3)	6.4(3)	834	535	
302.51(5)	3.9(2)	3.9(2)	535	233	
306.64(5)	54(2)	54(2)	307	0	*M*1/*E*2
388.9(1)	6.0(3)	22(1)	695	307	
407.2(1)	2.6(2)	2.6(2)	671	263	
417.44(5)	1.1(1)	1.1(1)	535	117	
438.1(1)[d,f,g,h]	0.7(1)		671	233	
466.69(5)[d,e,f]	24(1)	16(3)	467	0	
466.74(5)[e,f]	12.9(8)	40(3)	695	229	(*E*1)
480.4(1)[h]	1.0(2)		598	117	
516.1(1)[d,h]	1.1(2)		823	307	
524.1(1)[g,h]	2(1)		831	307	
527.4(1)	27(1)	31(2)	834	307	
534.80(6)	10.7(5)	13(1)	535	0	
553.2(1)	1.8(2)	1.7(2)	671	117	
559.5(1)[g,h]	0.9(1)		823	263	
570.70(7)	12.9(6)	21(1)	834	263	
590.3(1)[d]	0.9(1)	1.6(1)	823	233	
601.6(1)[d,f,g,h]	0.4(1)		834	233	
602.2(1)[f,g,h]	2.8(3)		831	229	
605.30(7)	12.3(5)	20(1)	834	229	
611.93(6)	7.0(4)	10(1)	729	117	
616.0(1)[f,g,h]	1.2(8)		1083	467	
618.5(1)[d,f]	2.3(8)		1085	467	
626.58(6)	23.2(9)	31(1)	660	33	
660.06(8)[f]	38(1)	50(5)	660	0	
662.1(1)[f]	24(1)	72(5)	695	33	
670.2(1)[d,f,g,h]	1.6(2)		934	263	
670.6(1)[f]	2.4(2)		671	0	
711.5(1)	0.9(1)				
729.23(7)	10.9(5)	13(1)	729	0	
756.7(1)	4.1(2)		1452	695	
776.06(7)[g,h]	1.6(4)		1083	307	
778.6(1)[d]	5.1(6)	5(1)	1085	307	
786.7(1)[d]	1.5(4)		1253	467	
792.1(1)	5.2(3)	9.8(5)	1452	660	
822.7(1)	4(2)	8(1)	823	0	
833(1)[d]	1.2(3)		1300	467	
834.0(1)	5.8(4)	9.4(3)	834	0	
837.1(1)	4.1(2)	4.7(2)	1101	263	
846.55(8)[g,h]	1.6(1)		1110	263	
852.7(1)[d,f,g,h]	2.2(3)		1085	233	
856.4(2)[d]	5.6(6)		1085	229	
868.2(1)	6.0(2)	7.1(3)	1101	233	
871.8(1)	4.2(2)	5.7(3)	1101	229	

TABLE I. (*Continued*).

Energy (keV)[a]	Intensity[b]		Placement		Multipolarity[c]
	^{143}Cs decay	^{144}Cs decay	From	To	
877.6(1)[g,h]	2.3(2)		1110	233	
880.5(1)[g]	1.0(1)				
890.0(1)[g,h]	1.1(1)		1154	263	
921.20(8)[d,g,h]	1.6(3)		1154	233	
933.75(8)[g,h]	1.5(1)		934	0	
971.1(2)[g,h]	1.2(1)		1204	233	
985.7(1)	1.8(1)		1452	467	
1020.8(1)[g]	2.1(2)		1253	233	
1024.5(1)	1.3(1)		1253	229	
1049.2(1)[g,h]	0.6(1)		1083	33	
1051.7(1)[f,g,h]	1.9(1)		1085	33	
1083.4(2)	2.8(1)		1083	0	
1100.8(1)[g,h]	1.0(1)		1101	0	
1153.6(1)	1.0(1)		1154	0	
1208.4(1)	2.0(3)		1441	233	
1219.9(1)	2.0(3)		1452	233	
1253.4(1)[g,h]	0.6(1)		1253	0	
1312.6(1)[g,h]	2.6(1)		1576	263	
1440.9(1)[g,h]	0.2(1)		1441	0	

[a]The uncertainties in the last digit are given in parentheses.
[b]For absolute intensity/100 decays multiply by 0.13±0.02 (Ref. 21). The uncertainties in the last digit(s) are given in parentheses.
[c]From Ref. 9.
[d]I_γ derived from coincidence data.
[e]I_γ corrected for daughter decay.
[f]Energy determined by subtracting initial and final level energies.
[g]Not previously observed.
[h]Not previously placed.

calculated by assuming a zero value for A_{44}. Large A_{44} values are quite unusual for cascades in odd-mass nuclides as

$$A_{44}=\delta_2^1 F_4(2,2,J_i,J)\delta_2^2 F_4(2,2,J_f,J)$$

and a small value for any of the four terms in this equation will quench the A_{44} term. In the case of ^{143}Ba, the F_4 terms for the transitions feeding the $\frac{5}{2}$ ground state are -0.61, 0.71, -0.40, 0.12, and -0.01 for intermediate levels of $\frac{1}{2}$, $\frac{3}{2}$, $\frac{5}{2}$, $\frac{7}{2}$, and $\frac{9}{2}$, respectively. The A_{22} coefficients given in Table III were corrected for the finite size of the detectors using the method outlined by Camp and Van Lehn.[17]

C. Beta branching and logft values

Upper limits for the beta branching and lower limits for the logft values for ^{143}Cs decay are reported in the decay scheme in Figs. 1(a) and (b). Because our study was aimed largely at the lower-lying levels in ^{143}Ba, no attempt was made to measure the complete γ-ray spectrum up to 6 MeV. As a result, the possibility of weak feeding to the levels by γ rays with energies greater than 2 MeV permits us to only report upper limits for the beta branching. It should be noted, however, that both previous decay studies did not have this restriction and neither reported any γ rays with energies greater than 2 MeV.

The limiting logft values were calculated from the compilation of Gove and Martin[18] with $Q_\beta=6.24\pm0.07$.[19] The beta branching to each level was calculated as the difference between the γ-ray and conversion electron transition intensity depopulating and populating each level. For the majority of transitions, the transition intensity was set equal to the γ-ray intensity as the conversion electron contribution is negligible. For the $M1/E2$ transitions for which the electron contribution could not be neglected, the transition intensity was set equal to the median value for a pure $M1$ and pure $E2$ transition as no definite mixing values could be assigned to the $M1/E2$ transitions; the measured conversion coefficients from Ref. 9 have an error of approximately 30%.

The difference in the ground state beta branch between our work (25%) and that of Schussler *et al.*[8] (78%) is due to the difference in the value used for the absolute intensity of the 195-keV γ ray in ^{143}Cs decay. Schussler *et al.* reported that the absolute intensity of the 195-keV γ ray is 3.3%. This value, however, is based upon an early measurement of the intensity of the 620-keV line in the daughter ^{143}La.[20] Sohnius *et al.* have since shown that the intensity of the 620-keV line in Ref. 20 was incorrect due to a false assumption about the operation of the ion source used in that experiment.[21] The absolute intensity of (12.6±1.9)% for the 195-keV γ ray used in this work

TABLE II. Results of the γ-ray coincidence scans for ^{143}Cs decay to levels of ^{143}Ba.

Gate (keV)	Gamma-ray peaks (keV) observed in the gate									
117	146	299	417	481	553	571	612			
146	117	407	571							
160	232	273	307							
195	78	238	466.74	602.2	605	757	856	872	1024	
229	466.74	605	856	872						
233	74	234	299	303	438	527	590	601.6	853	868
	878	921	971	1021	1208	1220				
234	233									
237	195	228	833							
263	407	559	571	670	836	847	890	1313		
273	160	389	516	524	527	776	778			
299	117	233	303	418	535					
303	233	299								
307	160	389	516	524	527	776	778			
388	273	307								
407	263									
417	117	299								
467*D*	195	229	616	619	757	787	833	986		
516	273	307								
524	273	307								
527	74	233	273	307						
535	299									
553	117									
559	263									
571	117	146	263							
590	233									
602*D*	195	233								
605	195	229								
612	117									
617*D*	160	195	233	234	237	263	273	307	466.69	
627	792									
660	792									
662	757									

was taken from the paper of Sohnius *et al.*[21] This value was determined by comparing the intensity of the 195-keV peak directly to the 293-keV peak in the granddaughter ^{143}Ce rather than to the 620-keV line in the daughter ^{143}La. The absolute intensity of the reference line in ^{143}Ce has been determined independently and in good agreement by several authors.

D. Construction of the decay scheme

The proposed decay scheme for ^{143}Ba is shown in Figs. 1(a) and (b). From our coincidence data, we are able to place elsewhere the γ rays that Schussler *et al.*[8] listed as evidence for the levels at 856 and 986 keV. The 856-keV γ ray is observed in coincidence with the 195- and 229-keV γ rays and the area of the 856-keV peak in these two gates accounts for the total singles intensity of the 856-keV transition. The 822-keV γ ray was observed in the singles spectra but there is no evidence which supports its feeding out of an 856-keV level. The 986-keV γ ray, which is reported to feed the ground state,[8] was observed in the 467-keV coincidence gate and as a result placed feeding out of the level at 1452 keV. And finally, the 753-keV γ ray which Schussler *et al.* placed as depopulating the 986-keV level was not observed in either this work or that of Rapport and Gayer.[9] If a 753-keV γ ray with an intensity unit of one does feed the level at 233 keV then it should have been easily observed as transitions with half this intensity were observed in the summed coincidence spectra.

In contrast to Schussler *et al.*,[8] the 467-keV γ ray is placed twice in the decay scheme. The area of the 467-keV peak in the 195- and 229-keV coincidence gates only accounts for 35% of the intensity of the 467-keV γ ray. Because all four of the transitions that feed the 467-keV level are observed in the 467-keV coincidence gate, we

TABLE III. Angular correlation coefficients for ^{143}Ba cascades.

Cascade	A_{22}[a]	χ^2
146-117	-0.12 ± 0.03	6.3
466-195	0.12 ± 0.02	8.3
571-263	0.06 ± 0.03	2.6
527-272	0.22 ± 0.01	5.8
527-306	0.04 ± 0.02	11

[a]Assuming $A_{44}=0$.

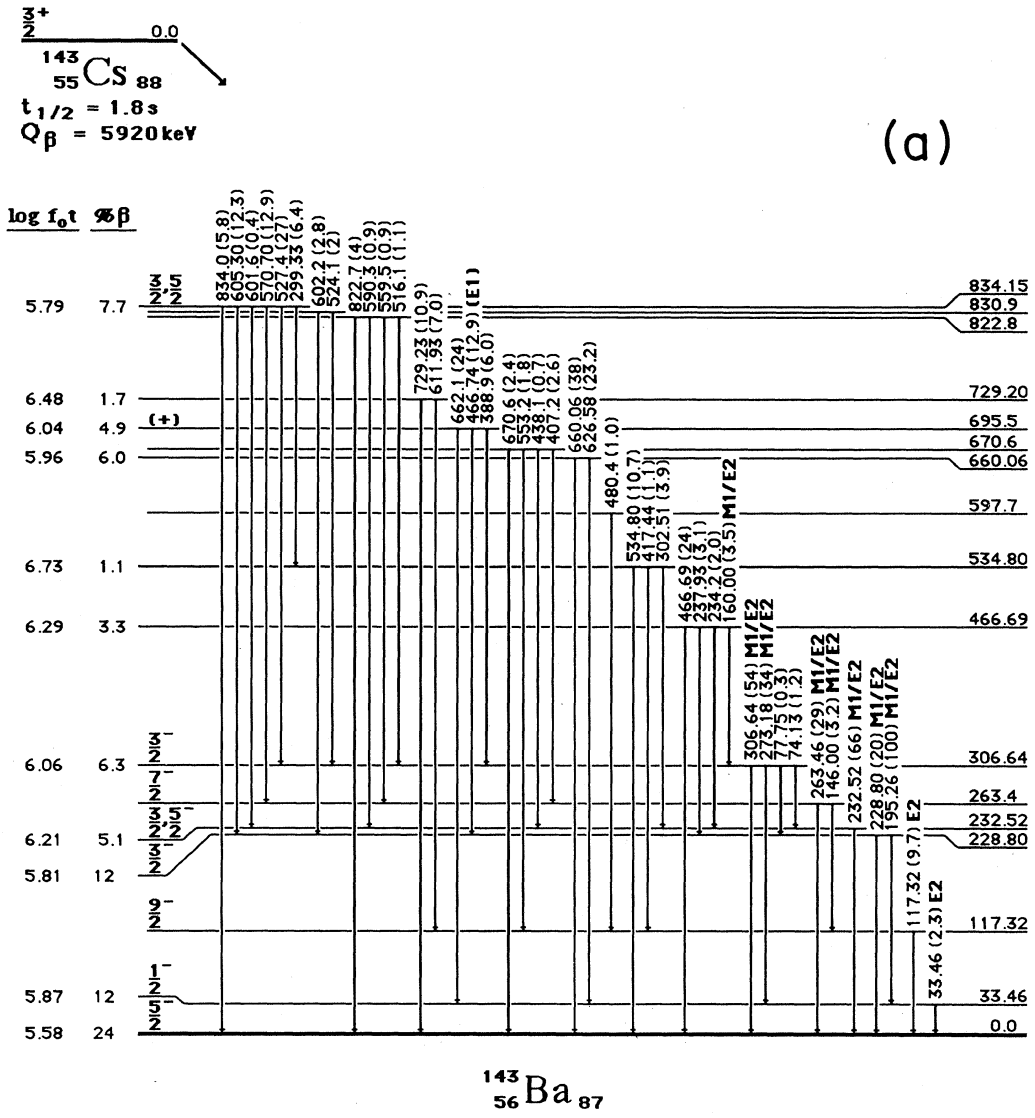

FIG. 1. (a) Part 1 of the level scheme proposed for ^{143}Ba. The transition multipolarities are from Ref. 9. (b) Part 2 of the level scheme proposed for ^{143}Ba.

conclude that there is a second 467-keV transition to the ground state.

Three γ rays observed in the singles spectra and placed in the decay scheme of Schussler *et al.* were not placed in the level scheme in this work. The 204-keV γ ray (466−263) was not observed in either the 146- or 263-keV coincidence gate. Likewise, the 712-keV γ ray (1452−729) was not observed in either the 729- or 612-keV coincidence gates and the 1083-keV γ ray (1312−229) was not observed in the 229- and 195-keV coincidence gates.

Nine new levels are proposed in our level scheme for ^{143}Ba. The level at 823 keV is supported by three coincidence cascades and the levels at 1110 and 1154 keV are supported by two coincidence cascades. The level at 1083 keV is supported by one coincident γ ray and two transitions feeding the ground state and 33-keV level. The level at 934 keV is supported by one γ-ray coincidence cascade and the 934-keV ground state transition. Because the other four new levels (598, 1300, 1441, and 1576 keV) are each supported by the observation of only one coincidence γ-ray cascade, their placement is tentative.

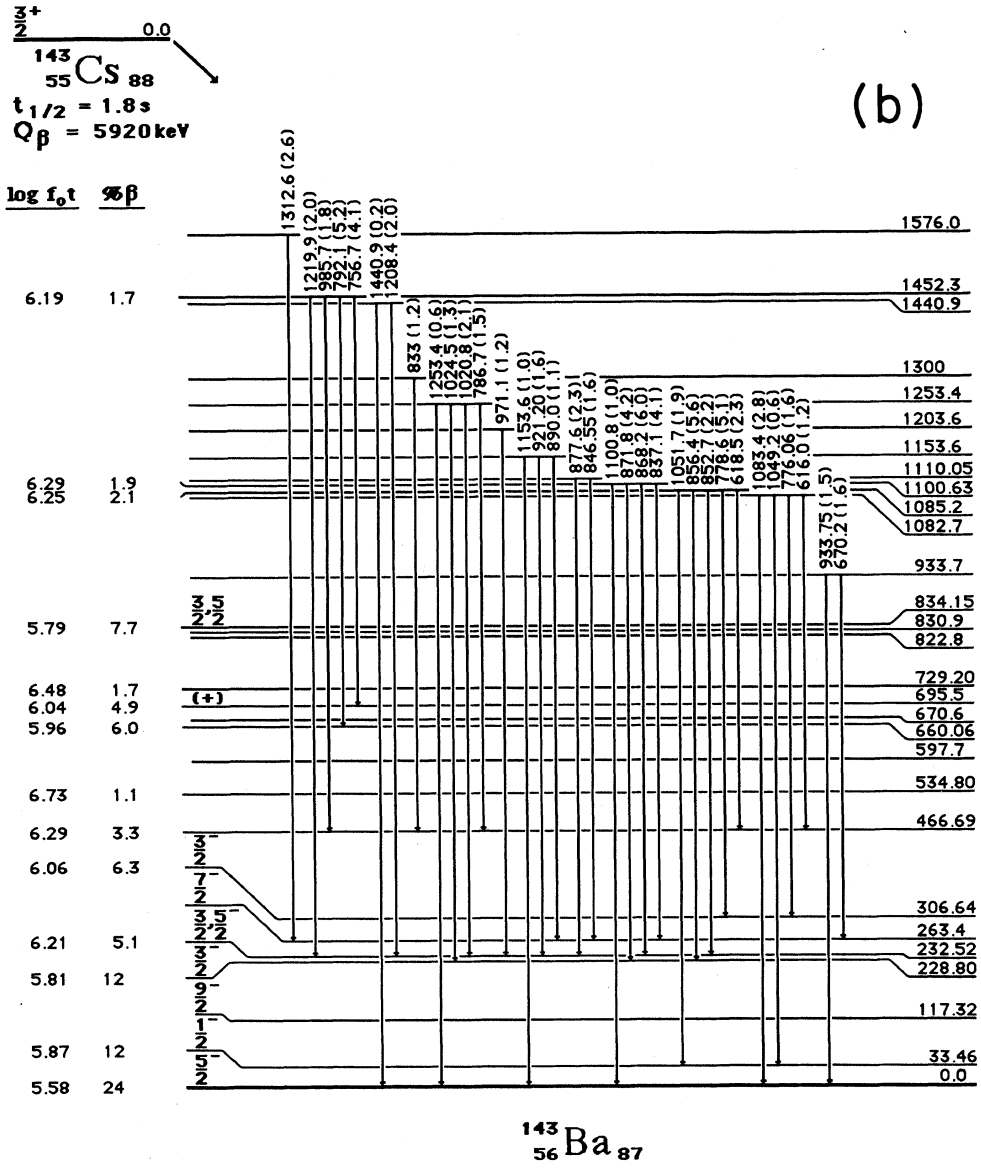

FIG. 1. (*Continued*).

E. Spin and parity assignments

1. The ground state

The ground state spin of ^{143}Ba has been measured[7] to be $\frac{5}{2}$. Negative parity is assigned to the ground state based upon the systematics of the $N=87$ isotones and the $Z=56$ isotopes. The ground state J^{π} assignments for the $N=87$ isotones from the $Z=64$ subshell closure are ^{151}Gd$=\frac{7}{2}^-$,[22] ^{149}Sm$=\frac{7}{2}^-$,[23] ^{147}Nd$=\frac{5}{2}^-$,[24] and ^{145}Ce $=(\frac{3}{2},\frac{5}{2})^-$.[25] Likewise, the ground state J^{π} assignments for the odd-A Ba isotopes from the $N=82$ closed shell are ^{139}Ba$=\frac{7}{2}^-$ and ^{141}Ba$=\frac{3}{2}^-$.[26,27] The deduced logft value of 5.6 for the ground state of ^{143}Ba is at the lower edge of the values expected for a first forbidden transition from a $\frac{3}{2}^+$ parent. This is, however, the lower limit for the ground state logft value and similar logft values for first forbidden transitions in this region are reported by Chung *et al.* in the study of the decay of ^{144}Ba to ^{144}La.[28]

The ground state of ^{143}Ba had been tentatively assigned positive parity.[15] This assignment is based upon an interpretation of the low-lying structure of ^{143}Ba in which the ground state is a member of a decoupled $K=\frac{1}{2}^+$ band built upon the $[660]\frac{1}{2}$ Nilsson orbital. However, recent data for the decay of ^{143}Ba to levels of ^{143}La support a negative parity assignment for the ground state of ^{143}Ba. Forty percent of the beta decay of ^{143}Ba feeds a level at 1010 keV in ^{143}La. Such a strong beta branch and corre-

sponding $\log f_0 t$ of 5.1 implies that this is an allowed transition and that the ground state of ^{143}Ba therefore has the same parity as the 1010-keV level in ^{143}La. The 1010-keV level, however, is known to have opposite parity of the ground state of ^{143}La as it depopulates to the 29-keV level in ^{143}La via an $E1$ transition which in turn depopulates to the ground state via an $M1$ transition. Inasmuch as Faller *et al.*[16] have shown that the ground state J^π assignment for ^{143}La is $\frac{7}{2}^+$, the ground state parity of ^{143}Ba must be negative.

2. The 33-keV level

The $E2$ multipolarity of the 33-keV transition[9] limits the ground state J^π of the 33-keV level to a range of $\frac{1}{2}^- - \frac{9}{2}^-$. However, the strong beta feeding to this level would not be possible for either a $\frac{7}{2}^-$ or $\frac{9}{2}^-$ level from a $\frac{3}{2}^+$ parent. The 33-keV level was tentatively assigned a spin of $\frac{1}{2}^-$ based upon the assumption that it would be quite unlikely for either a $\frac{3}{2}^-$ or $\frac{5}{2}^-$ level to be able to feed the $\frac{5}{2}^-$ ground state by a transition in which the $M1$ component is completely suppressed.[8] The $\frac{1}{2}^-$ assignment is consistent with the systematics of the $N=87$ isotones[22] as a $\frac{1}{2}^-$ state drops from 576 keV in ^{151}Gd to below 100 keV in ^{145}Ce.[29]

3. The 117-keV level

Like the 33-keV level, the $E2$ multipolarity of the 117-keV transition[9] limits the J^π of the 117-keV level to a range of $\frac{1}{2}^- - \frac{9}{2}^-$. A $\frac{1}{2}^-$ spin assignment is, however, ruled out by the nonzero A_{22} value found for the 146–117 cascade (Table III). If the assumption used for making the $\frac{1}{2}^-$ assignment to the 33-keV level is valid, then the 117-keV level most likely has a spin of $\frac{9}{2}^-$. Support for such an assignment is found in both the absence of a direct branch to this level and the lack of a γ-ray branch to the $\frac{1}{2}^-$ 33-keV level. The A_{22} angular correlation coefficient of -0.122 for the 146-117 cascade is consistent with a $\frac{7}{2}^-(M1/E2)\frac{9}{2}^-(E2)\frac{5}{2}^-$ cascade (see below) with the multipole mixing ratio δ for the 146-keV $M1/E2$ transition ranging from 0 to 0.05. Note that such a small δ^2 term for the $M1/E2$ transition reduces the A_{44} coefficient to a value well below our limits of uncertainty.

4. The 229- and 306-keV levels

The spin and parity of both the 229- and 306-keV levels are determined by the multipolarity of the two transitions which depopulate each of these levels. The $M1/E2$ multipolarity of the 229- and 306-keV ground state transitions[9] limits the J^π of the 229- and 306-keV levels to $\frac{3}{2}^-$, $\frac{5}{2}^-$, or $\frac{7}{2}^-$. Moreover, the $M1/E2$ multipolarity of the 195- and 273-keV transitions to the $\frac{1}{2}^-$ 33-keV level limits the J^π of the 229- and 306-keV levels to $\frac{1}{2}^-$ or $\frac{3}{2}^-$. As a result, the J^π assignment for both the 229- and 306-keV levels must be $\frac{3}{2}^-$ as this is the only overlap between the two cases. The absence of any γ-ray feeding from these two $\frac{3}{2}^-$ levels to the 117-keV level is further support for the $\frac{9}{2}^-$ spin assignment to the 117-keV level.

5. The 263-keV level

Like the 229- and 306-keV levels, the J^π of the 263-keV level is determined by the multipolarity of the two transitions which depopulate it. The $M1/E2$ multipolarity of the 263-keV ground state transition[9] limits the spin of the 263-keV level to $\frac{3}{2}^-$, $\frac{5}{2}^-$, or $\frac{7}{2}^-$. Moreover, the $M1/E2$ multipolarity of the 146-keV transition[9] which feeds the $\frac{9}{2}^-$ 117-keV level limits the spin of the 263-keV level to $\frac{7}{2}^-$, $\frac{9}{2}^-$, or $\frac{11}{2}^-$. As a result, the J^π of the 263-keV level must be $\frac{7}{2}^-$ as this is again the only overlap between the two cases. The lower limit for the $\log f_1 t$ of 8.8 is, within experimental error, consistent with a $\frac{7}{2}^-$ assignment and a first forbidden unique transition from a $\frac{3}{2}^+$ parent.

6. The 695-keV level

The intensities shown in Table I for the γ rays arising from the delayed-neutron population of the low-energy levels of ^{143}Ba are approximately equal to those observed in the beta decay of ^{143}Cs. The one exception is the 695-keV level which appears to be considerably more strongly populated by delayed-neutron emission from excited negative parity levels in ^{144}Ba. In view of the fact that the delayed-neutron emission occurs from a large number of levels with spins and parities of 0^-, 1^-, and 2^- with highly mixed configurations, the population of the final levels is largely statistical. An important source of distinction that could enhance the population for the 695-keV level would be a parity change which would require the emission of a p-wave neutron. If s-wave neutron emission is hindered because of the complex structure of these low-energy negative parity levels, then the p-wave emission could be favored to the positive parity level. The conversion coefficient determined by Rappaport and Geyer for the 467-keV doublet ($\alpha_K=0.75$) is below either the $M1$ ($\alpha_K=1.14$) or $E2$ ($\alpha_K=0.99$) value, indicating that the weaker of the two components of the doublet is likely an $E1$ ($\alpha_K=0.14$) transition. Consequently, we have made a tentative assignment of positive parity for the 695-keV level.

7. The 834-keV level

Because the 834-keV level feeds both a $\frac{3}{2}^-$ level and a $\frac{7}{2}^-$ level, its spin can range from $\frac{3}{2}^-$ to $\frac{7}{2}^-$; any other values would imply that one of the transitions from the 834-keV level would have ΔJ greater than 2. The spin of $\frac{7}{2}$, however, can be ruled out by the A_{22} value of 0.215 ± 0.012 for the 527-273 cascade; A_{22} is always less than or equal to 0.14 for a $\frac{7}{2}(E2)\frac{3}{2}(M1/E2)\frac{1}{2}$ cascade (A_{44} is always zero for any cascade with an intermediate spin of $\frac{3}{2}$). In addition, the lower limit for the $\log f_1 t$ of 7.8 is well below the value of 9 expected for a first forbidden unique transition from a $\frac{3}{2}^+$ parent to a $\frac{7}{2}^-$ level.

TABLE IV. Gamma rays assigned to the decay of ^{147}La.

Energy (keV)[a]	Intensity[b]	Placement From	Placement To	Energy (keV)[a]	Intensity[b]	Placement From	Placement To
69.09(8)	3.8(5)	187	118	377.49(8)[d]	2.3(1)	495	118
117.70(8)	100	118	0	382.6(1)[c]	1.8(2)	598	215
141.8(2)[c]	1.2(3)	495	353	387.94(7)	4.8(2)	505	118
152.3(1)[c]	0.9(4)	505	353	399.33(5)	20.3(9)	517	118
156.10(7)	5.1(6)	274	118	402.46(5)	12(5)	402	0
156.7(1)	< 1			410.9(1)	5.7(5)	598	187
159.2(2)	5.3(6)	598	438	416.5(1)[d]	0.6(1)	770	353
170.2(2)	< 1	609	438	432.95(9)[c]	1.2(3)	786	353
184.4(1)[c]	4(1)	517	333	437.2(2)[d]	2.7(1)	770	333
186.80(5)	54(1)	187	0	438.17(3)[d]	42(2)	438	0
207.5(1)	0.2(5)	609	401	461.8(1)[c]	1.1(2)	677	215
215.0(1)[c]	23(2)	333	118	469.1(1)	< 1	907	438
215.3(3)[c]	4.4(8)	402	187	480.0(2)[c]	0.8(4)	598	118
215.4(3)	29(2)	215	0	490.52(6)	1.6(2)	677	187
217.6(1)[c]	3.2(3)	433	215	495.17(3)	8.1(5)	710	215
225.0(1)[c]	3.4(1)			506.2(1)[c]	0.1(1)	907	401
235.55(5)	20.6(1)	353	118	507.61(5)[c]	8.5(1)	625	118
246.39(9)	3.1(5)	433	187	516.99(5)	10.3(7)	517	0
272.47(3)[c]	0.5(1)			520.0(1)[c]	0.2(1)	921	401
273.8(1)[c]	19(4)	274	0	523.55(9)	3.2(3)	710	187
279.9(1)	3.9(8)	495	215	557.79(5)	4.8(4)	832	274
283.41(5)	23(1)	401	118	570.75(6)	9.5(7)	786	215
290.06(8)[d]	2.2(1)	505	215	571.1(1)[c]	0.6(2)	924	353
292.9(2)[d]	2.2(1)	625	333	599.2(1)	10(2)	786	187
308.56(7)	2.8(3)	495	187	601.8(1)	5(2)		
318.69(8)[d]	3.9(5)	505	187	644.99(6)	3.2(3)	832	187
320.47(6)[c]	4.6(9)	438	118	647.4(3)	0.9(1)	921	274
332.8(1)	4.8(7)	333	0	674.66(5)	3.8(2)		
334.8(1)	3.0(4)	609	274	713.1(1)	0.7(2)		
353.22(3)	15(1)	353	0				

[a]The uncertainties in the last digit of the energy values are given in parentheses.
[b]The uncertainties in the last digit(s) of the intensity values are given in parentheses.
[c]I_γ taken from coincidence gates.
[d]I_γ corrected for daughter or ^{146}La decay.

IV. ^{147}Ce EXPERIMENTAL RESULTS

A. Gamma-ray energies and intensities

The γ rays assigned to ^{147}La decay are listed in Table IV and the coincidences in Table V. The assignments were based upon the appearance of the γ ray in (1) the ^{147}La singles spectra and (2) the coincidence spectra gated on the strongest transitions whose half-lives have been previously determined.[24] No γ-ray peaks from the ^{147}Cs grandparent were observed in the singles spectra and only the strongest line from the ^{147}Ba parent was observed in the singles spectra. The contribution of the ^{147}Ce daughter γ rays to the ^{147}La singles spectra was removed using the intensity values reported by Schussler *et al.*[12] In addition, the intensities of several transitions were corrected for ^{146}Ba decay using the relative intensity values in Ref. 30. The ^{146}Ba interference comes from the (26.4±3.7)% delayed-neutron branch in ^{147}Cs decay.[31] For the majority of the γ rays given in Table IV, the energy and intensity values were determined from the singles data. In several cases, however, it was impossible to ascertain this information from the singles spectra because the intensity of the transition was too low or the γ ray was a member of a complex multiplet. In these instances, the energy and/or intensity values were determined from the coincidence spectra.

In order to determine the absolute intensity values of the γ rays, an $A=147$ radioactive sample in which the 13-min ^{147}Pr had reached saturation was produced by allowing the beam to accumulate at the parent port of the MTC for two hours. The γ-ray singles spectrum containing the $A=147$ isobars in equilibrium was then accumulated and the intensities of the strongest lines attributed to each decay were determined. A similar experiment was performed by Sohnius *et al.*[21] and our results for the

TABLE V. Results of the γ-ray coincidence scans for ^{147}La decay to levels of ^{147}Ce.

Gate (keV)	Gamma-ray peaks (keV) observed in the gate									
69	118									
97	118									
118	69	97	156	207	215	225	236	272	283	320
	377	388	399	433	480	491	508	520		
156	118	402								
159	438									
187	215	246	309	319	411	491	511	524	587	599
	645									
207	118	283								
215*T*	118	156	184	186	215	218	225	280	290	293
	383	437	462	495	511	558	570.8			
225	118	215								
236	118	142	152	215	416	433	438	571.1		
246	118	187								
272	118	283								
274	333	558								
280	215									
283	118	144	207	226	272	506	520			
290	215									
293	118	215								
309	187									
319	118	187								
320	118									
333	225	437								
335	156	274								
353	142	152	416	433	571.1					
377	118	215								
388	118									
399	118									
402	94	156								
411	187	293								
433	118	236	353							
437/438	236	469	511	667						
491	118	187								
495	215									
506	118	283								
508	118									
524	187									
570.8/571.1	215	236	353							
599	187									
645	187									

relative transition intensities of the strongest lines from $A=147$ La, Ce, and Pr decay are in good agreement with their reported values. In order to convert these relative transition intensities to absolute values, the absolute intensity of one or more of the γ rays in ^{147}Pr must be known. Two values, however, differing by almost a factor of 2 have been reported in the literature for the 315-keV transition in ^{147}Pr decay. Pinston *et al.*[32] report a value of 12.6% whereas Harmatz and Ewbank[24] report a value of 24%. Because the value reported by Pinston *et al.* gives an inordinately large value for the ground state beta branch of ^{147}La decay (see below), we use the value reported by Harmatz *et al.* to calculate the absolute γ-ray intensities.

B. Construction of the decay scheme

The proposed decay scheme for ^{147}Ce is shown in Fig. 2. Like Schussler *et al.*,[12] we find evidence of three 215-keV transitions in ^{147}La decay and a 215-keV level in ^{147}Ce. A 215-keV transition is seen in both the 118- and the 187-keV coincidence gates. The area of the 215-keV peak in these two gates, however, only accounts for 48% of the total intensity of the 215-keV γ ray. This, coupled with the fact that five of the peaks in the 215-keV coin-

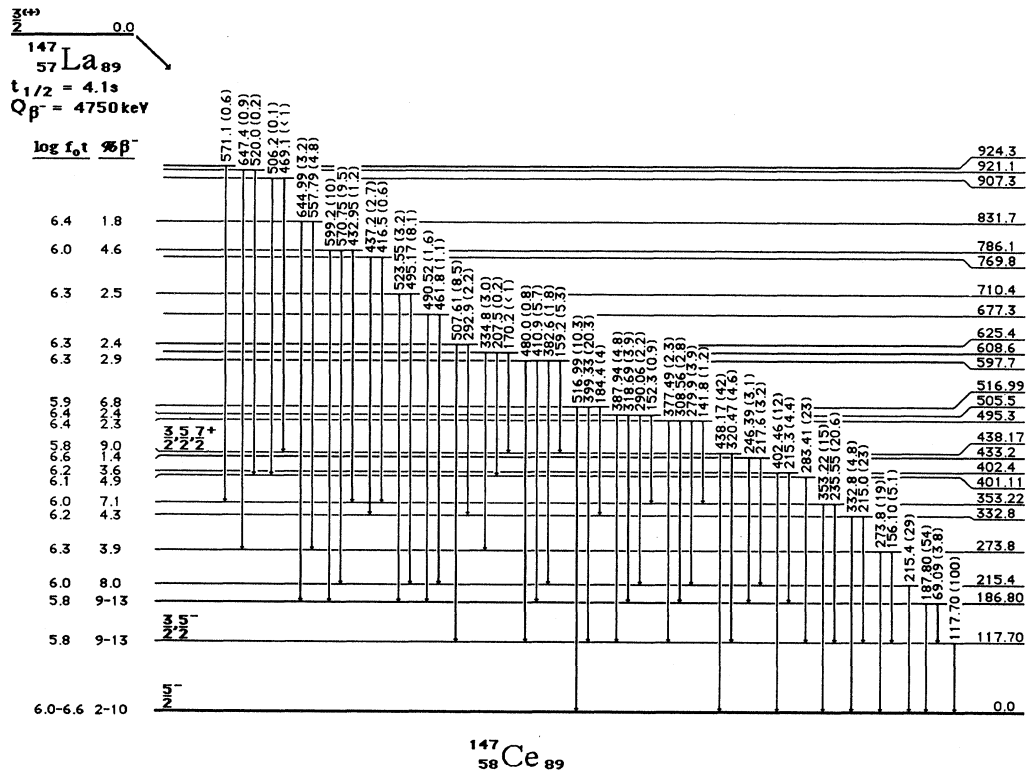

FIG. 2. The level scheme proposed for ^{147}Ce.

cidence spectrum are not seen in either the 118-keV gate or the 187-keV gate, indicates that there is a third 215-keV transition to the ground state.

In addition to the 215-keV level, we also find evidence for the levels at 433, 608, 677, and 710 keV that were proposed by Schussler *et al.*[12] but not by Shmid *et al.*[11] As can be seen from Fig. 2, the 433-, 608-, and 710-keV levels are supported by at least two coincidence cascades. In contrast to Ref. 12, a 359-keV level is not placed in ^{147}Ce; a 359-keV transition was not observed in any of the singles spectra. Likewise, no evidence was found for the 97-keV γ ray from the 215-keV level to the 118-keV level. This transition, which is reported to have a relative transition intensity of 6, should have been readily observed as the 69-keV transition with only four intensity units was easily seen in the 118-keV coincidence gate. And finally, of the five tentative transitions reported in Ref. 12, only the 292-keV γ ray was confirmed in this work.

Two new levels are proposed for ^{147}Ce: a 598- and a 770-keV level. The 598-keV level is supported by the appearance of the 411-keV peak in the 187-keV coincidence gate and the 383-keV peak in the 215-keV coincidence gate. Likewise, the 770-keV level is supported by the appearance of a 416-keV peak in both the 353- and 235-keV coincidence gates and the appearance of a 437-keV peak in both the 333- and 215-keV coincidence gates.

C. Beta branching

The beta branching and logft values calculated for ^{147}La decay are directly dependent upon the absolute intensities of the transitions from ^{147}La decay. Table VI summarizes the beta branching and logft values found using the two different absolute γ-ray intensity values for the 315-keV transition in ^{147}Pr decay. The logft values were calculated from the compilation of Gove and Martin[18] with $Q_\beta = 4.75 \pm 0.12$ MeV.[33] The beta branch to each level was calculated as the difference between the transition intensity depopulating and populating each level. For the majority of transitions, the intensity was set equal to the γ-ray intensity as the conversion-electron contribution is negligible. The conversion coefficients reported by Schussler *et al.* were used to calculate the transition intensity for the 118- and 187-keV γ rays.[12] The theoretical coefficient for a pure $M1$ transition was used to calculate the transition intensities for the two strongest 215-keV γ rays. Although Schussler *et al.* report that these two transitions are $E2$ and $M1/E2$, any $M1$ or $E2$ admixture in the transitions will not change the intensities as the conversion coefficients for pure $M1$ and pure $E2$ transitions are equal at 215 keV. The limits for the beta branching to the 118- and 186-keV levels were calculated assuming that the conversion coefficient for the 69-

TABLE VI. Beta branching and logft values for ^{147}La decay.

Level (keV)	% beta[a]	Logf_0t	% beta[b]	Logf_0t
0.0	47–51	5.2	2–10	6.0–6.6
117.70	5–7	6.1	9–13	5.8
186.80	5–7	6.1	9–13	5.8
215.4	4.4	6.2	8.0	6.0
273.8	2.1	6.5	3.9	6.3
332.8	2.4	6.5	4.3	6.2
353.22	3.9	6.2	7.1	6.0
401.11	2.7	6.4	4.9	6.1
402.4	2.0	6.5	3.6	6.2
433.2	0.8	6.9	1.4	6.6
438.17	4.9	6.1	9.0	5.8
495.3	1.2	6.7	2.3	6.4
505.5	1.3	6.6	2.4	6.4
516.99	3.7	6.2	6.8	5.9
597.7	1.6	6.5	2.9	6.3
608.6	0.5	7.1	0.8	6.8
625.4	1.3	6.6	2.4	6.3
677.3	0.2	2.4	0.4	7.1
710.4	1.4	6.5	2.5	6.3
769.8	0.4	7.0	0.7	6.8
786.1	2.5	6.2	4.6	6.0
831.7	1.0	6.6	1.8	6.4
907.3	0.1	7.7	0.1	7.4
921.1	0.1	7.4	0.2	7.2
924.3	0.1	7.7	0.1	7.4

[a]Assuming I_{abs} for 315-keV γ ray in ^{147}Pr decay is 0.126±0.004 (Ref. 32).
[b]Assuming I_{abs} for 315-keV γ ray in ^{147}Pr decay is 0.24±0.01 (Ref. 24).

keV transition ranged from 3.5 (pure $M1$) to 8.0 (pure $E2$). Because a ground state beta branch of 50% is unlikely in that it is one order of magnitude higher than the ground state beta branches observed in all the other nearby nuclides, our spin and parity assignments and subsequent discussion are based upon the beta branching calculated from the 24% absolute intensity value[24] for the 315-keV γ ray in ^{147}Pr.

D. Spin and parity assignments

1. The ground state

A spin and parity of $\frac{5}{2}^-$ is assigned to the ground state of ^{147}Ce based upon the systematics of the region. The ground state J^π assignments for the $N=89$ isotones are ^{151}Sm$=\frac{5}{2}^-$,[34] ^{149}Nd$=\frac{5}{2}^-$,[35] and ^{145}Ba$=\frac{5}{2}^-$.[2] Likewise, the ground state J^π assignments for the odd-A $Z=58$ Ce isotopes are ^{141}Ce$=\frac{7}{2}^-$,[36] ^{143}Ce$=\frac{3}{2}^-$,[37] and ^{145}Ce $=(\frac{3}{2},\frac{5}{2})^-$.[25] Although no spin and parity have been assigned to the ground state of the parent, systematics from the work of Faller[38] suggest that ^{147}La has a ground state J^π of $\frac{3}{2}^+$. This assignment, as can be seen from Fig. 3, is consistent with the great similarity observed between the structures of ^{145}Ba and ^{147}Ce and the great similarity observed between the beta branching in the decays of ^{145}Cs and ^{147}La.

2. The 118-keV level

If the spin of the ground state is $\frac{5}{2}^-$, then the $M1/E2$ multipolarity of the 118-keV transition reported in Ref. 12 limits the spin and parity of the 118-keV level to $\frac{3}{2}^-$, $\frac{5}{2}^-$, or $\frac{7}{2}^-$. A spin of $\frac{7}{2}^-$ is, however, unlikely because of the large beta branch to the 118-keV level. If ^{147}La does have a ground state spin of $\frac{3}{2}^+$, then the observed logft value would have to approach nine to be consistent with a $\frac{7}{2}$ spin assignment for the 118-keV level.

3. The 187-keV level

The $E2$ multipolarity of the 187-keV transition[12] implies that the 187-keV level has a spin ranging from $\frac{1}{2}^-$ to $\frac{9}{2}^-$. Again, however, the large beta branch to this level makes a $\frac{7}{2}^-$ or $\frac{9}{2}^-$ assignment unlikely if the parent has a spin of $\frac{3}{2}^+$.

4. The 438-keV level

The spin and parity of the 438-keV level is limited to $\frac{3}{2}^+$, $\frac{5}{2}^+$, or $\frac{7}{2}^+$ by the $E1$ multipolarity of the 438-keV γ ray.[12] The logft of 5.8 is consistent with an allowed beta transition from a $\frac{3}{2}^+$ parent and a spin assignment of either $\frac{3}{2}^+$ or $\frac{5}{2}^+$ to the 438-keV level.

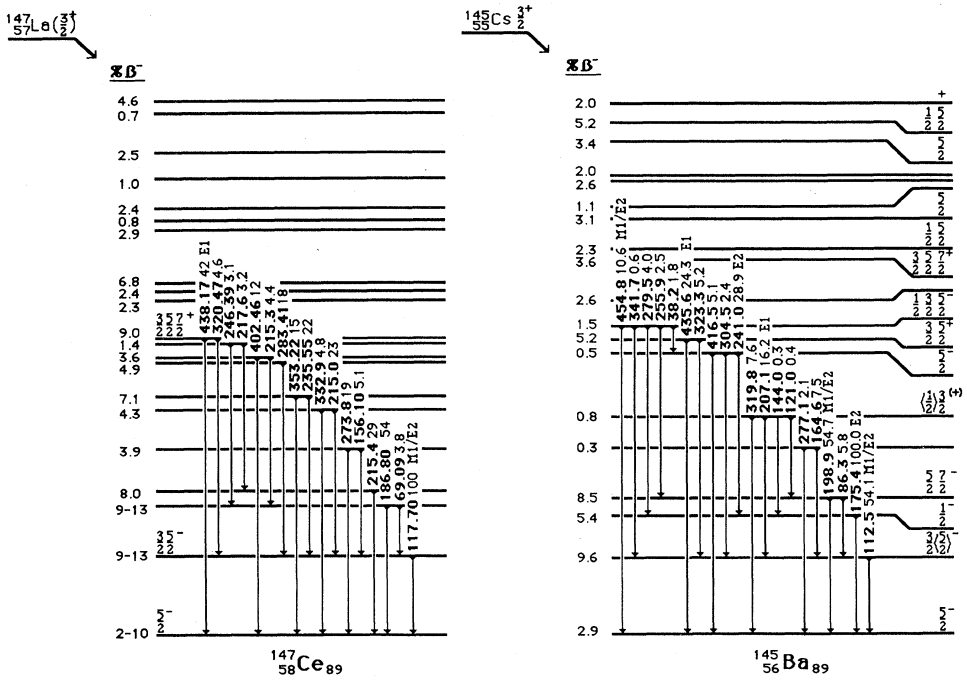

FIG. 3. A comparison of the low-lying level structure observed in ^{145}Ba and ^{147}Ce. The transition multipolarities for ^{147}Ce are from Ref. 12. The ^{145}Ba level scheme is from Ref. 2.

V. DISCUSSION

A. The $N=87$ isotones

The systematics of the $N=83$ isotones are shown in Fig. 4, along with the levels of the even-even $N=82$ closed shell core nuclides. The systematics of the $N=85$ isotones are shown in Fig. 5, along with the levels of the even-even $N=84$ core nuclides. The systematics of the $N=87$ isotones are shown in Fig. 6 along with the systematics of the $N=86$ even-even core nuclei. A close examination of Figs. 5 and 6 reveals that the structures of the $N=87$ isotones ^{153}Dy, ^{151}Gd, and ^{149}Sm evolve directly from the single neutron structure for the $N=83$ nuclides through the $(f_{7/2})^3$ structures in the $N=85$ isotones. On the other hand, the structures of ^{147}Nd, ^{145}Ce, and ^{143}Ba bear progressively less resemblance to their respective $N=85$ and $N=83$ isotopes (Figs. 4 and 5). The energy gap observed in the level structure of the $N=85$ isotones (Fig. 5) and the higher mass $N=87$ isotones (Fig. 6) has disappeared. Moreover, the first $\frac{9}{2}^-$ level, which lies above 600 keV in ^{141}Ba, has dropped to 117 keV in ^{143}Ba and the $\frac{1}{2}^-$ level identified in ^{143}Ce and ^{145}Nd at 862 and 920 keV, respectively, has dropped to 214 keV in ^{147}Nd and lies near the ground state in both ^{145}Ce and ^{143}Ba. It should be cautioned at this point that this structure change rests on the assumption that the observed low-lying pure $E2$ transitions imply $\Delta J=2$ rather than $\Delta J=1$ where the $M1$ component has, for some reason, been significantly hindered. Both the $\frac{1}{2}^-$ and $\frac{9}{2}^-$ levels in ^{143}Ba and the $\frac{1}{2}^-$ level in ^{145}Ce rest on this assumption. If, however, these are stretched $E2$ transitions, then it is clear that the addition of two neutrons to these $N=85$ isotones results in a significant change in the nuclear structure. Similarly, a large structural change is also observed in the odd-proton nuclides in this region at $N=86$. Like the $N=85$ and $N=87$ isotones, the low-lying structures of the odd-Z $N=84$ and $N=86$ isotones are very similar near the $Z=64$ subshell closure. The $N=86$ isotones ^{141}Cs and ^{143}La, however, reveal structural features that are simply not present in the $N=84$ isotones ^{139}Cs and ^{141}La.[16,39]

Meyer *et al.*[40] have proposed that the low-lying structure of the $N=87$ isotones can be accounted for in terms of a coexisting $(f_{7/2})^{-3}$ cluster and a quasideformed $h_{9/2}$ band. The levels identified with the cluster and $h_{9/2}$ band are shown in Fig. 7 and it is interesting to note that the tentative $\frac{9}{2}^-$, 117-keV level in ^{143}Ba, of which Meyer *et al.* had no knowledge, is consistent with the evolution of the proposed $h_{9/2}$ band. The one serious difficulty with this interpretation of the structure of the $N=87$ isotones is, however, that the downward trend of the $h_{9/2}$ single particle orbital towards ^{143}Ba (Fig. 7) runs counter to the systematics of the $N=83$ and $N=85$ isotones. The position of the $h_{9/2}$ orbital changes little as Z changes across the $N=83$ isotones as shown in Fig. 4, and the $h_{9/2}$ single particle strength drops, not toward $Z=56$, but towards $Z=64$ across the $N=85$ isotones as shown in Fig. 5. In both the $N=83$ and 85 isotones, the $h_{9/2}$ orbital drops sharply beyond $Z=64$ in response to the filling of the

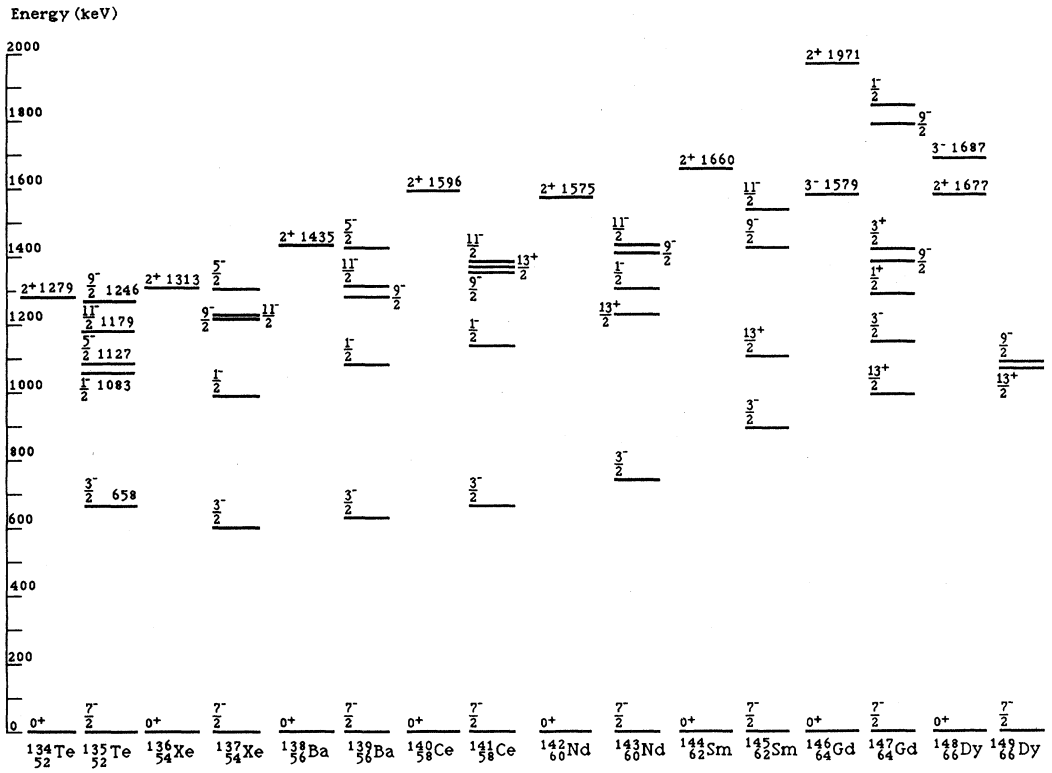

FIG. 4. The systematics of the $N=83$ isotones plotted along with the low-lying levels in the $N=82$ even-even core nuclides.

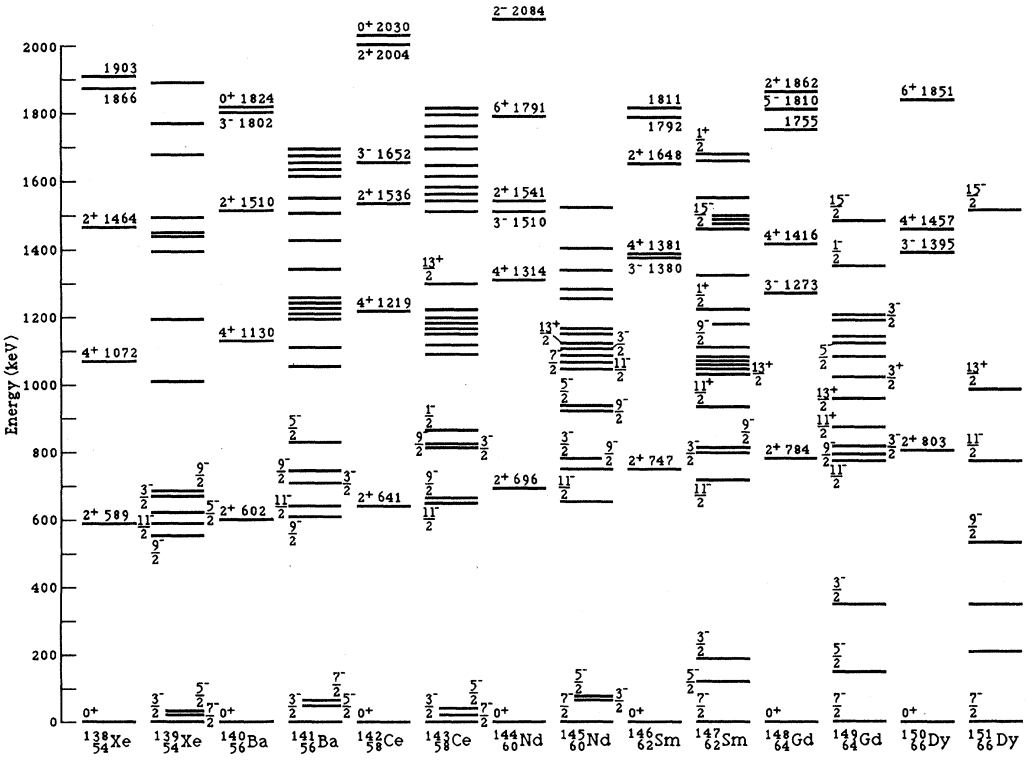

FIG. 5. The systematics of the $N=85$ isotones plotted along with the low-lying levels in the $N=84$ even-even core nuclides.

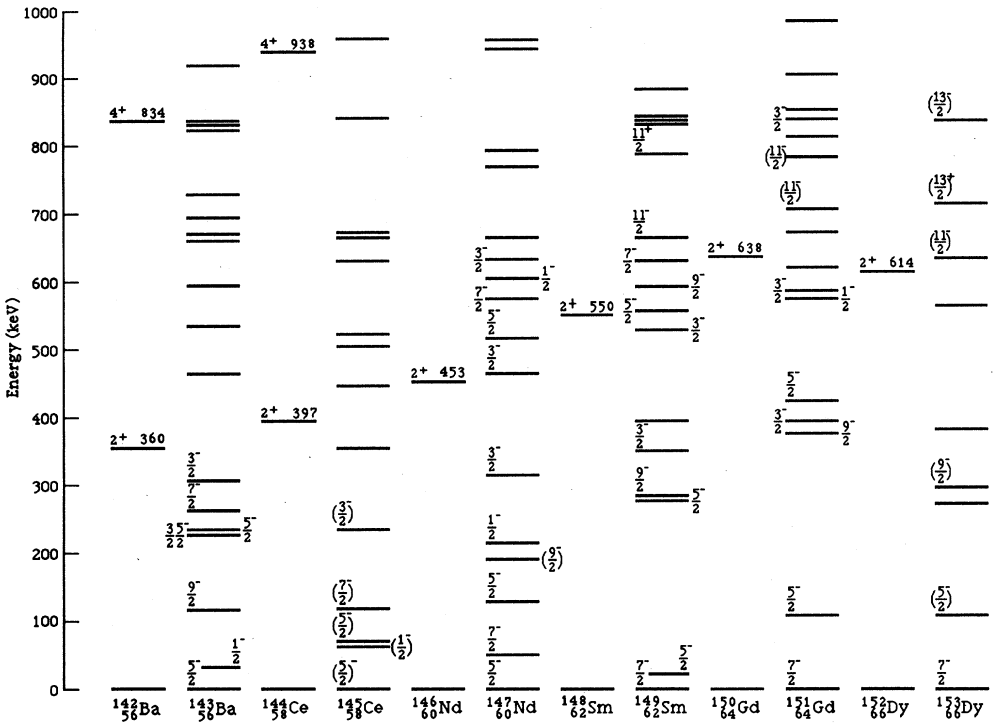

FIG. 6. The systematics of the $N=87$ isotones plotted along with the low-lying levels in the $N=86$ even-even core nuclides.

$h_{11/2}$ proton spin-orbit partner orbital. The idea that the $h_{9/2}$ single particle orbital does not drop sharply towards $Z=56$ in the $N=87$ isotones is also supported by the $(^3\mathrm{He},\alpha)$ pickup reaction on ^{148}Sm and ^{150}Sm. The two $\frac{9}{2}^-$ levels in ^{149}Sm at 286 and 591 keV show very similar parameters to the two $\frac{9}{2}^-$ levels in ^{147}Sm at 809 and 1108 keV in that the pickup strength to the lower level in both nuclides is approximately 0.6 and the pickup strength to the upper $\frac{9}{2}^-$ level is negligible.[41] Because the pickup strength only changes from 0.53 in ^{147}Sm to 0.60 in ^{149}Sm, there is little evidence to indicate that the 500-keV drop in position of the $\frac{9}{2}^-$ level has been induced by additional $h_{9/2}$ single particle character.

In addressing the $J-2$ anomaly observed in the $N=85$ isotones, Vanden Berghe and Paar[42] also showed that a $J+1$ anomaly could occur if the coupling strength between the $(f_{7/2})^3$ cluster and the quadrupole phonon was significantly increased. They did not, however, show the effects that increased coupling would have on the entire level scheme. Thus we would suggest that it is quite possible that the low-lying level structure observed in ^{143}Ba can be accounted for in terms of an $(f_{7/2})^{-3}$ cluster coupled to the quadrupole phonon. The domination of the cluster configuration in ^{143}Ba and ^{145}Ce, as compared to ^{149}Sm, ^{151}Gd, and ^{153}Dy where the coexistence of the cluster and $h_{9/2}$ band has been well demonstrated,[40] could be attributed to the large drop in energy of the 2^+ phonon from 638 keV in ^{150}Gd to 360 keV in ^{142}Ba. Moreover, the lowering of the $\frac{5}{2}^-$ and $\frac{9}{2}^-$ members of the cluster, rather than the $\frac{3}{2}^-$ and $\frac{5}{2}^-$ members as in the $N=85$ isotones, could result from (1) increased coupling strength and (2) the fact that the cluster is now generated by neutron holes in the $f_{7/2}$ orbital. The difficulty with this interpretation of the structure of ^{143}Ba and ^{145}Ce is the low-lying $\frac{1}{2}^-$ level. In contrast to the $\frac{9}{2}^-$ level, even strong coupling does not account for the $\frac{1}{2}^-$ level as it is impossible to construct a spin $\frac{1}{2}$ state from an $(f_{7/2})^{-3}$ cluster.

An alternative approach to the low-lying structure of the lighter mass $N=87$ isotones is to treat the low-lying levels in terms of the Nilsson model. The three lowest levels in ^{143}Ba can be grouped into a decoupled $K=\frac{1}{2}^-$ rotational band with a rotational parameter of 19 keV and a decoupling parameter of 4.9. The large rotational parameter is consistent with the lack of well-defined rotational bands in ^{143}Ba and ^{145}Ce and the vibrational appearance of the core nuclides ^{142}Ba and ^{144}Ce; the ratio of the energy of the first 4^+ level to the energy of the first 2^+ level in both core nuclides is 2.3. In addition, the measured quadrupole moment[7] for the ground state of ^{143}Ba indicates that the ground state is a member of a Nilsson band with $K<\frac{5}{2}$. Two major difficulties are, however, encountered in this interpretation of the structure of ^{143}Ba. First of all, the $\frac{3}{2}^-$ and $\frac{7}{2}^-$ members of the proposed band are predicted to be at 368 and 780 keV, respectively. As can be seen from the proposed decay

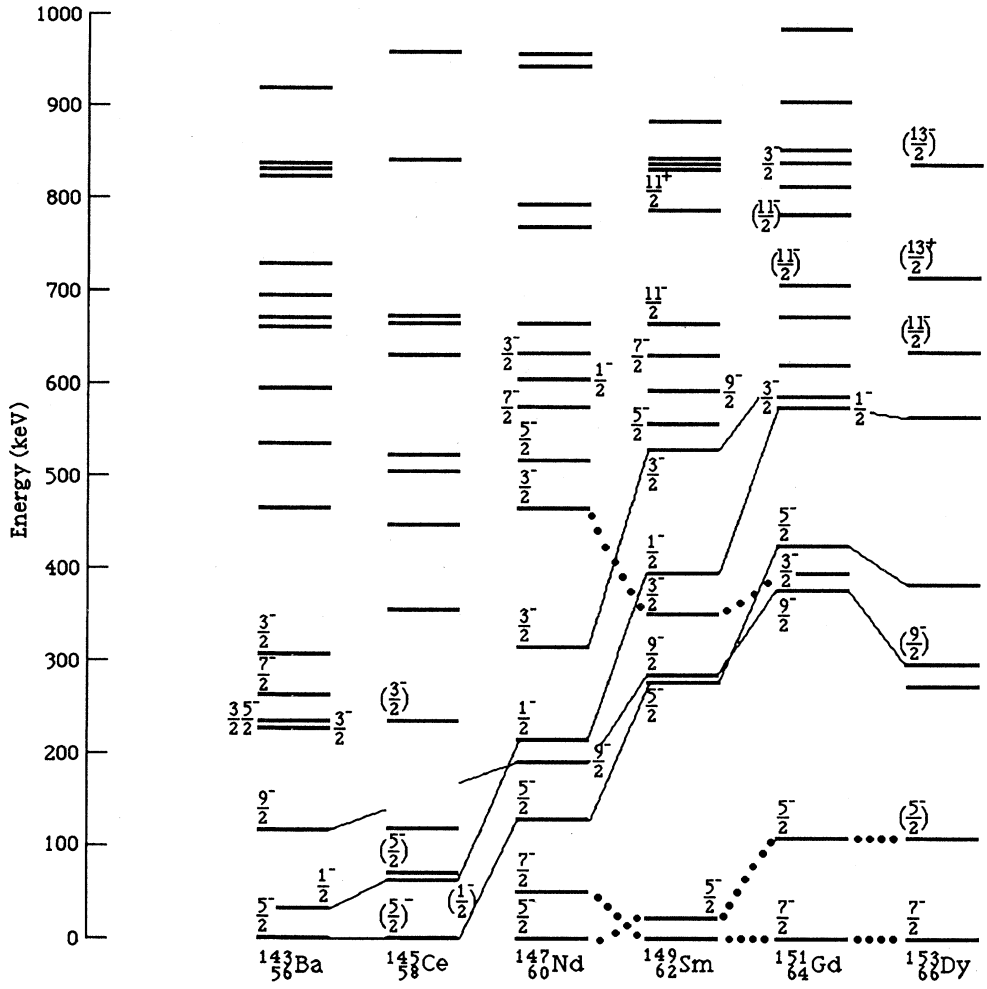

FIG. 7. The systematics of the $N=87$ isotones showing the members of the $(f_{7/2})^{-3}$ cluster (dotted line) and quasideformed $h_{9/2}$ band (solid line) proposed by Meyer *et al.* (Ref. 40).

scheme, no level is observed in ^{143}Ba between 729 and 823 keV and the $\frac{3}{2}^-$ level is approximately 60 keV below the expected value. Secondly, the decoupling parameter of 4.9 is only consistent with a $K=\frac{1}{2}^-$ band built upon the $[541]\frac{1}{2}$ Nilsson orbital.[43] Yet, in calculations where reflection asymmetry is both included and neglected, the $[541]\frac{1}{2}$ orbital lies well below the Fermi surface in this region and is not a plausible candidate for the $K=\frac{1}{2}$ band.

In their paper, Mueller *et al.* point out that the ground state spin, spectroscopic quadrupole moment, and magnetic dipole moment of ^{143}Ba can be accounted for by core-quasiparticle calculations based upon the quadrupole deformed Nilsson model.[7] In this approach, the ground state of ^{143}Ba is represented by a mixture of low-Ω orbitals from the $f_{7/2}$ and $h_{9/2}$ levels whose dominant components at $\beta_2\approx 0.22-0.27$ would be the highly decoupled $[530]\frac{1}{2}$ orbital and the $[532]\frac{3}{2}$ Nilsson orbital. These two orbitals lie near the Fermi surface in ^{143}Ba at β_2 deformations greater than 0.13. Addition of reflection asymmetry to such Nilsson calculations does not greatly alter the position of these two orbitals and is, hence, also consistent with the measured spins and moments.

B. The $N=89$ isotones

The systematics of the $N=89$ isotones are shown in Figs. 8(a) and 8(b) along with the systematics of the low-lying states in the $N=90$ even-even core nuclides. Without further experimental work and definite spin and parity assignments, the most important conclusion to be drawn from this work is the remarkable similarity between the low-lying structure of ^{145}Ba and ^{147}Ce as shown in Fig. 3. Moreover, if ^{145}Ba does lie in the center of a region of weak reflection-asymmetric deformation, this similarity suggests that the new region is sharply bounded. Recently Phillips *et al.* have shown that, in contrast to ^{146}Ce, the even-even Ce isotopes with $N\geq 90$ do not become octupole deformed at high spins as they do not show the alternating parity bands with members connect-

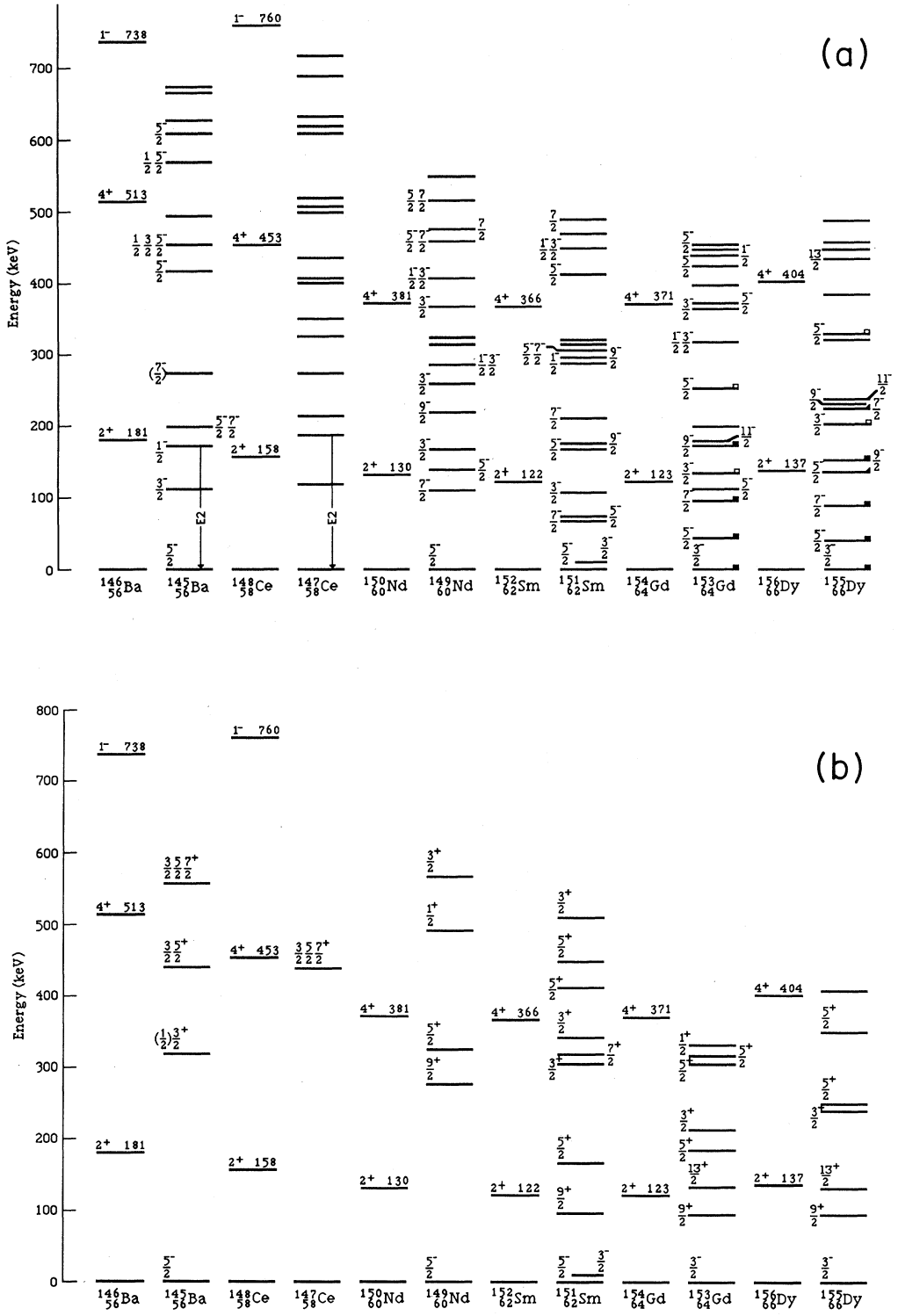

FIG. 8. (a) The systematics of the negative parity states in the $N=89$ isotones plotted along with the low-lying levels in the $N=90$ even-even core nuclides. (b) The systematics of the positive parity states in the $N=89$ isotones plotted along with the low-lying levels in the $N=90$ even-even core nuclides.

ed by strong $E1$ transitions.[4] (This result was predicted by the cranked mean field calculations of Nazarewicz.[44]) Yet, if ^{145}Ba does break reflection symmetry in the intrinsic frame, then the similarity between it and ^{147}Ce would indicate that ^{147}Ce may also be octupole deformed and that the predicted island of reflection-asymmetric deformation in this region includes only ^{145,146,147}Ce with a sharp cutoff between $N=89$ and $N=90$ for the Ce isotopes.

In contrast to the $N=85$ and $N=87$ isotones, the systematics of the $N=89$ isotones do not exhibit effects from the $Z=64$ subshell closure. The appearance of clear rotational structure in ^{153}Gd and ^{155}Dy and the decrease in the density of levels across the $N=89$ isotones from $Z=64$ to $Z=56$ suggests that the heavier $N=89$ isotones are more deformed than ^{145}Ba and ^{147}Ce. This would indicate that the occupancy of the $h_{9/2}$ neutron orbital is great enough at $N=89$ to induce the deformation observed in the even-even nuclides with $N \geq 90$.

VI. CONCLUSION

The level structures of ^{143}Ba and ^{147}Ce have been investigated. Spins and parities have been assigned to the levels in ^{143}Ba based upon the measured angular correlation coefficients and logft values and the reported internal conversion coefficients. The level scheme proposed for ^{147}Ce resolves the discrepancies between the two previous works. Tentative spins and parities have been proposed for a few of the levels in ^{147}Ce based upon the systematics of the $N=89$ isotones and the reported transition multipolarities.

These new data extend and complete the systematics of the $N=87$ and 89 isotones, and permit an evaluation of the remarkable and significant changes in structure that occur with the addition of each pair of neutrons beyond the $N=82$ closed shell. The magnetic dipole and electric quadrupole moments measured for the odd-mass Ba nuclides can be contrasted with the slightly smaller quadrupole moments and larger dipole moments for the odd-A Xe nuclides[45] and interpreted to indicate that maximum deformation for nuclides with $Z \leq 64$ and $N \leq 90$ occurs for the Ba nuclides.[46] The disappearance of octupole structure at low energies that appears to take place between ^{147}Ce and ^{148}Ce marks the boundary between a region of deformation in which octupole and quadrupole deformations play approximately equal roles and a region in which quadrupole deformation is dominant. That two regions exist has been well demonstrated by Casten[47] in his Fig. 12. Subsequently, Casten, Brenner, and Haustein[48] suggested that deformation as generally observed throughout the chart of nuclides requires about eight valence protons and eight valence neutrons beyond double magic nuclides. For this mass region, that would occur precisely at ^{148}Ce. For the nuclides with $Z<64$, the data for the low-energy levels in the odd-neutron nuclides are not yet well enough established to distinguish between calculations that either do or do not include octupole contributions. In contrast, however, the $\frac{3}{2}^+$ ground states for the odd-mass ^{143,145}Cs nuclides as well as the alternating parity bands in both the odd-neutron and even-even Xe, Ba, and Ce nuclides can only be understood by including a contribution from octupole deformation.[1] The new data presented here, the new in-beam data[3,4] for the even-even Ba and Ce nuclides, prospective magnetic moment data for the La and Pr nuclides, and prospective new fission fragment deexcitation data offer a solid basis for more detailed calculations in which the contributions from several sources of deformation can be evaluated and the extent to which reflection-asymmetric deformations influence the observed structures of these nuclides can be established. Included in these possible structures will be those described by Iachello and Jackson that involve cluster structure in which the large cluster is double magic ^{132}Sn and the small cluster consists of the 10–18 additional nucleons in the nucleus.[49]

ACKNOWLEDGMENTS

This work was supported by the Office of High Energy and Nuclear Physics of the U.S. Department of Energy under Contract DE-AS05-79ER10494 with the University of Maryland and through Brookhaven National Laboratory under Contract DE-AC02-76CH00016. The authors appreciate the assistance of Dr. R. L. Gill and Dr. A. Piotrowski and the TRISTAN technical staff during the performance of these experiments and the subsequent reduction of the data as well as the hospitality of Dr. R. F. Casten and the entire Neutron Nuclear Physics Group at Brookhaven National Laboratory.

*Present address: Department of Chemistry, University of Kentucky, Lexington, KY 40506.

†Present address: Las Vegas Environmental Monitoring Systems Laboratory, U.S. Environmental Protection Agency, Las Vegas, NV 89193.

‡Present address: Center for Analytical Chemistry, National Institute of Standards and Technology (formerly the National Bureau of Standards), Gaithersburg, MD 20899.

[1] G. A. Leander, W. Nazarewicz, P. Olanders, I. Ragnarsson, and J. Dudek, Phys. Lett. **152B**, 284 (1985).

[2] J. D. Robertson, S. H. Faller, W. B. Walters, R. L. Gill, H. Mach, A. Piotrowski, E. F. Zganjar, H. Dejbakhsh, and R. F. Petry, Phys. Rev. C **34**, 1012 (1986).

[3] W. R. Phillips, I. Ahmad, H. Emling, R. Holzmann, R. V. F. Janssens, T. L. Khoo, and M. W. Drigert, Phys. Rev. Lett. **57**, 3257 (1986).

[4] W. R. Phillips, R. V. F. Janssens, I. Ahmad, H. Emling, R. Holzmann, T. L. Khoo, and M. W. Drigert, Phys. Lett. B **212**, 402 (1988).

[5] W. Urban, R. M. Lieder, W. Gast, G. Hebbinghaus, A. Kramer-Flecken, K. P. Blume, and H. Hubel, Phys. Lett. B **185**, 331 (1987).

[6] W. Urban, R. M. Lieder, W. Gast, G. Hebbinghaus, A. Kramer-Flecken, T. Morek, T. Rzaca-Urban, W. Nazarewicz, and S. L. Tabor, Phys. Lett. B **200**, 424 (1988).

[7] A. C. Mueller, F. Buchinger, W. Klempt, E. W. Otten, R. Neu-

gart, C. Ekstrom, and J. Heinemeier, Nucl. Phys. **A403**, 234 (1983).
[8]F. Schussler, J. Blachot, E. Monnand, B. Fogelberg, S. H. Feestra, J. van Klinken, G. Jung, and K. D. Wunsch, Z. Phys. A **290**, 359 (1979).
[9]M. S. Rapaport and A. Gayer, Int. J. Appl. Radiat. Isot. **36**, 689 (1985).
[10]J. Blachot, H. P. Bocquet, E. Monnand, B. Pfeiffer, F. Schussler, H. Lawin, T. A. Khan, W. D. Lauppe, G. Sadler, H. A. Selic, and K. Sistemich, Kernforschungsanlage Jülich Report No. KFA-IKP-10/77, 1977 (unpublished), p. 49.
[11]M. Shmid, Y. Y. Chu, G. M. Gowdy, R. L. Gill, H. I. Liou, M. L. Stelts, R. E. Chrien, R. F. Petry, H. Dejbakhsh, C. Chung, and D. S. Brenner, in *Proceedings of the 4th International Conference on Nuclei Far From Stability,* edited by P. G. Hansen and O. B. Nielsen (Skolen, Helsingor, 1981), pp. 576–580.
[12]F. Schussler, B. Pfeiffer, H. Lawin, J. Munzel, J. A. Pinston, and K. Sistemisch, in *Proceedings of the 4th International Conference on Nuclei Far From Stability,* edited by P. G. Hansen and O. B. Nielsen (Skolen, Helsingor, 1981), pp. 589–597.
[13]R. L. Gill and A. Piotrowski, Nucl. Instrum. Methods A **234**, 213 (1985).
[14]A. Piotrowski, R. L. Gill, and D. C. McDonald, Nucl. Instrum. Methods **224**, 1 (1984).
[15]L. K. Peker, Nucl. Data Sheets **48**, 753 (1986).
[16]S. H. Faller, J. D. Robertson, E. M. Baum, C. Chung, C. A. Stone, and W. B. Walters, Phys. Rev. C **38**, 307 (1988).
[17]D. C. Camp and A. L. Van Lehn, Nucl. Instrum. Methods **76**, 192 (1969).
[18]N. B. Gove and M. J. Martin, Nucl. Data Tables **10**, 205 (1971).
[19]U. Keyser, F. Munnich, B. Pahlmann, and B. Pfeiffer, Z. Phys. A **300**, 249 (1981).
[20]J. Blachot, S. Dousson, E. Monnand, F. Schussler, and B. Fogelberg, J. Phys. Lett. **37**, 275 (1976).
[21]B. Sohnius, M. Brugger, H. O. Denschlag, and B. Pfeiffer, Radiochim. Acta **37**, 125 (1984).
[22]B. Harmatz, Nucl. Data Sheets **19**, 33 (1976).
[23]G. E. Holland, Nucl. Data Sheets **19**, 337 (1976).
[24]B. Harmatz and W. B. Ewbank, Nucl. Data Sheets **25**, 113 (1978).
[25]E. M. Baum, J. D. Roberston, P. F. Mantica, S. H. Faller, C. A. Stone, W. B. Walters, R. A. Meyer, and D. F. Kusnezov, Phys. Rev. C **39**, 1514 (1989).
[26]L. K. Peker, Nucl. Data Sheets **32**, 1 (1981).
[27]L. K. Peker, Nucl. Data Sheets **45**, 69 (1985).
[28]C. Chung, W. B. Walters, R. L. Gill, M. Shmid, R. E. Chrien, and D. S. Brenner, Phys. Rev. C **26**, 1198 (1982).
[29]B. Pfeiffer, F. Schussler, J. Blachot, S. J. Feenstra, J. van Klinken, H. Lawin, E. Monnand, G. Sadler, H. Wollnik, and K. D. Wunsch, Z. Phys. A **287**, 191 (1978).
[30]C. Chung, W. B. Walters, D. S. Brenner, R. L. Gill, M. Shmid, Y. Y. Chu, R. E. Chrien, L. J. Yuan, F. K. Wohn, and R. A. Meyer, Phys. Rev. C **31**, 2199 (1985).
[31]P. L. Reeder, Brookhaven National Laboratory Report No. BNL-51778, 1983 (unpublished), p. 358.
[32]J. A. Pinston, R. Roussille, G. Bailleul, J. Blachot, J. P. Bocquet, E. Monnand, B. Pfeiffer, H. Schrader, and F. Schussler, Nucl. Phys. **A246**, 395 (1975).
[33]R. Stippler, F. Munnich, H. Schrader, K. Hawerkamp, R. Decker, B. Pfeiffer, H. Wollnik, E. Monnand, and F. Schussler, Z. Phys. A **285**, 287 (1978).
[34]W. B. Cook, M. W. Johns, G. Lovhøiden, and J. C. Waddington, Nucl. Phys. **A259**, 461 (1976).
[35]J. A. Pinston, R. Roussille, G. Sadler, W. Tenten, J. P. Bocquet, B. Pfeiffer, and D. D. Warner, Z. Phys. A **282**, 303 (1977).
[36]J. K. Tuli, Nucl. Data Sheets **23**, 529 (1978).
[37]J. K. Tuli, Nucl. Data Sheets **25**, 603 (1978).
[38]S. H. Faller, Ph.D. thesis, University of Maryland, 1986 (unpublished).
[39]S. H. Faller, P. F. Mantica, E. M. Baum, C. Chung, J. D. Robertson, C. A. Stone, and W. B. Walters, Phys. Rev. C **38**, 905 (1988).
[40]R. A. Meyer, J. T. Meadows, and E. S. Macias, J. Phys. G **8**, 1413 (1982).
[41]J. Reckstad, G. Lovhøiden, J. R. Lien, S. El Kazzaz, C. Ellegaard, J. Bjerregaard, P. Knudsen, and P. Kleinheinz, Nucl. Phys. **A348**, 93 (1980).
[42]G. Vanden Berghe and V. Paar, Z. Phys. A **294**, 183 (1980).
[43]J. M. Irvine, *Nuclear Structure Theory* (Pergamon, New York, 1972), p. 333.
[44]W. Nazarewicz, in *Proceedings of the International Conference on Nuclear Structure Through Static and Dynamic Moments,* edited by H. H. Bolotin (Conference Proceedings Press, Melbourne, 1987), p. 180.
[45]W. Borchers, E. Arnold, W. New, R. Neugart, K. Wendt, G. Ulm, and the ISOLDE Collaboration, Phys. Lett. B **216**, 7 (1989).
[46]D. Kusnezov and F. Iachello, Phys. Lett. B **209**, 420 (1988).
[47]R. F. Casten, Nucl. Phys. **A443**, 1 (1985).
[48]R. F. Casten, D. S. Brenner, and P. E. Haustein, Phys. Rev. Lett. **58**, 658 (1987).
[49]F. Iachello and A. D. Jackson, Phys. Lett. **B108**, 151 (1982).